DYNAMOMETRIC PROVING RING WITH NONCONSTANT GEOMETRICAL CHARACTERISTICS OF ITS CROSS-SECTIONS

Dimitar Petrov[1], Dimitar Dimitrov[1]
[1]Technical University –Sofia, branch Plovdiv, Plovdiv, Bulgaria
e-mail: dimgog@abv.bg, ddimitrov_tu@abv.bg

Abstract: This work presents the work of studying separately by means of a theoretical approach and by means of three dimensional modeling (by CAD) of the characteristic - diametrical deformation depending on the diametrical load of a dynamometric ring whose cross-section is not constant in its geometry. The way to obtain this dependence through the theoretical approach is demonstrated by applying the method of numerical integration of the expressions obtained by applying the second Castigliano's theorem in order to find the displacement of the point of application of concentrated force in the direction of its line of action. Also given are the results of the simulation loading of the 3-D model of the investigated ring. Finally, these all results are compared with the experimental ones and some conclusions are made.
Key words: proving ring, deflection characteristic with respect to applied force, Castigliano's second theorem

INTRODUCTION

It is well known that dynamometric proving rings are devices for measuring forces [1]. The dynamometric rings are of different sizes [2] (figure 1a). They are made of alloy steel and their production includes rough machining of forged blanks, thermo-treatment and precise grinding to the final size and roughness of their surfaces. In general every such device consists of two main elements, the elastic ring itself and the diameter-measuring system located in the center of the ring [1][2]. Forces are applied to the ring through the external bosses. The resulting change in diameter, referred to as the deflection of the ring, is measured with a measuring system presented here (Figure 1 b) by a precision micrometer and the vibrating reed mounted diametrically within the ring. The concept and design [1] of proving rings (Figure 1-b) were created originally by Whittmore and Petrenko at the (US) National Bureau of Standards (now called the National Institute of Standards and Technology). To measure the diameter of the ring, the reed is inserted into the vibration mode by tapping it with a pencil slightly. As the reed vibrates, the micrometer screw is adjusted until the tip of the spindle begins to touch the free end of the vibrating reed by extinguishing vibrations. The touch generates a buzzing sound [2], and this is the time to take into account the change of the diameter of the ring. This technique provides repetitive and stable indications with an accuracy of about 1 ÷ 2μm [3]. Nowadays, in the newer systems with dynamometric proving rings, the micrometer and the reed after Whittmore&Petrenko's design are replaced by a built-in metering dial indicator, by a set of electrical resistive strain gauges using a Wheatstone bridge, or by a video camera and software for ring size measurement.

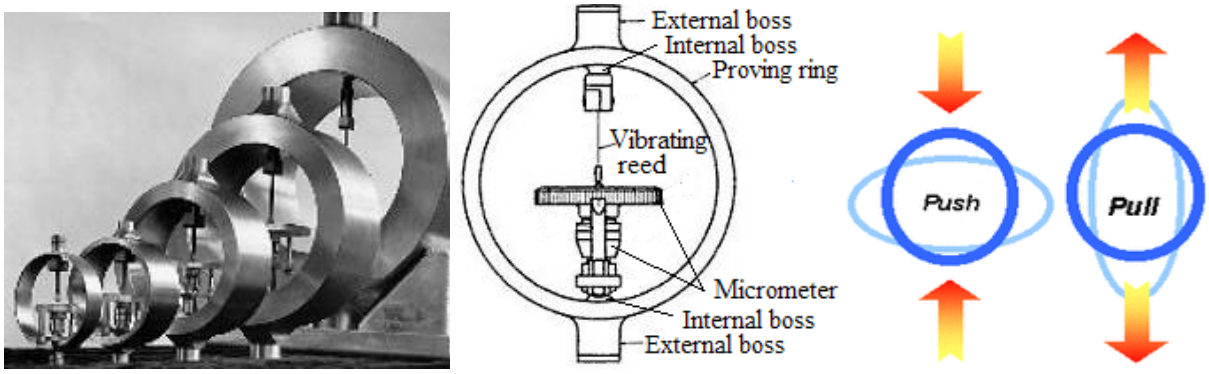

Figure 1. a) Proving rings in a variety of sizes; **b)** Schematic of a proving ring having external bosses for attachment and internal bosses and the precision deflection-measuring system presented with a micrometer and a vibrating reed; **c)** Proving ring deflections at compression or tension forces.

The proving rings (Figure 1-c) can be used and can be designed to measure compressive forces, tensile forces, or both types of forces. In particular, the tensile force measuring rings [2] are most often made with external threaded bosses and are provided with pulling rods which are screwed into the bosses. Typically, the proving rings are designed to have a deflection of about 0.84 mm to 4.24 mm and are designed in such way to have the relative measurement uncertainty from 0.075% to about 0.0125%.
When loading with the forces for measuring in the rings internal forces arise - bending, shearing and tension, which change along the circular perimeter of the rings. These internal forces can be determined by applying the so-called general theorems of Strength of Materials (e.g. of Castigliano and this of Menabrea) [4], [5], [6]. For example, at load of a thin circular ring according to Figure 2-a, the diagrams of distribution of normal internal force, tangential internal force, and bending moment will respectively be as shown in Figure 2-b, Figure 2-c and Figure 2-d (see [6], page 533).

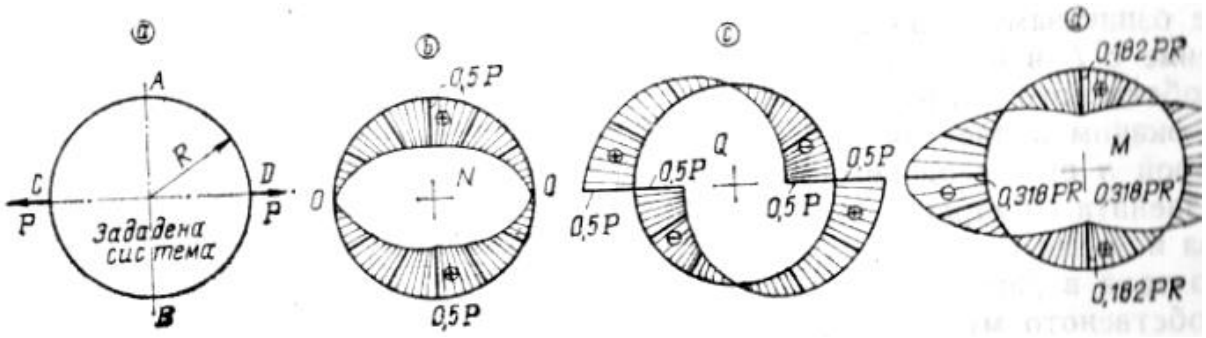

Figure 2. Thin planar circular ring [6, page 533] a) Load scheme; b) Diagram of distribution of the normal internal force; c) Diagram of distribution of the tangential internal force; d) Bending moment distribution diagram.

It is stated in the literature that the bending moment is decisive both for the strength ([7], page 89) and for the magnitude of the deformation ([5], page 170), whereas the influence of the other two internal forces (normal and tangential) is negligible. As the bending moment changes (as it could be seen from its diagram of distribution- Figure 2-d) under a certain periodic law on the circumference of the ring, it could be applied the principle of designing with the uniform strength. According this principle the geometric resistivity characteristics (section modules) of the cross-sections of the ring should be designed to be proportional (on permissible structural degree) to their corresponding internal forces (in this case the bending moment). In the case of a circular proving ring, the maximum bending moments are in the cross-sections passing through the line of applying of the measured two opposing forces as well as through the perpendicular of that direction (see Figure 2-d), whereas the bending moments in the segments of the ring between these two directions are minimal.

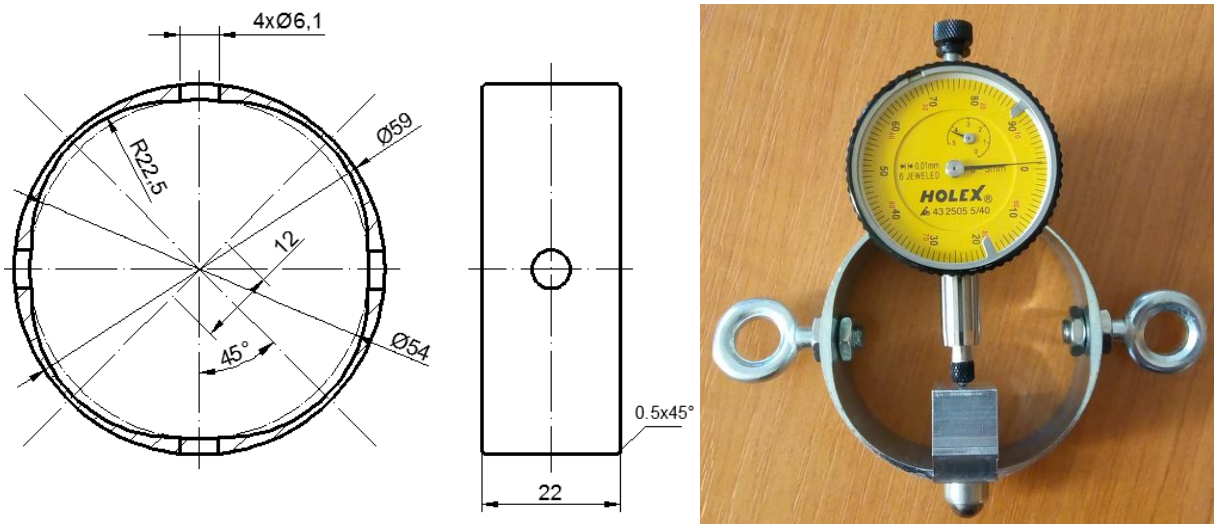

a b

Figure 3. Design sketch (a) and realization (b) of a dynamometric proving ring.

This gives rise to the idea of constructing and testing a force measuring ring (Fig. 3) with non-uniform cross-section, which under conditions of guaranteed strength provides greater elastic flexibility of the ring and hence its greater sensitivity as a measuring element. Similar designs are known in the literature [8]. In the design under consideration, the aim is to create an elastic element composed of simple and technologically easy to implement surfaces - cylindrical and planar.
In this work are presented the theoretical and model 3D-CAD characteristics of the investigated dynamometric ring and these characteristics are compared with each other and then they are compared to experimentally obtained one.

THIN PROVING RING WITH CONSTANT CROSS SECTION

Internal forces induced by load with diametrical compressive forces

By the name “thin ring” is meant a ring (Figure 4-a) whose dimensions of the cross-section (h = 2.5 mm) in radial direction are negligible in comparisone to the diameter (∅59 mm), and under a ring with constant (or invariable) cross-section is meant a ring, whose cross-section has constant dimensions (here h = 2.5 mm and b = 22 mm). The proving ring has to bear load both compressive and tensile . In here case, let the load is with two equal opposite compressive diametral forces. To determine the internal forces and the elastic characteristic "Diametral deflection - Load", the general theorems from Strength Of Materials can be used - the Castigliano's second theorem which state that first partial derivative of the total internal energy in the structure (in case here - the proving ring) with respect to the force applied at any point is equal to the deflection at the point of application of that force in the direction of its line of action and the Menabrea theorem that the first partial derivative of potential energy U of a elastic body with respect to statically indeterminate in internal force (in case here - the bending moment X1) is zero (Eq.1)(because internal forces do not carry out any work).

$$(\delta U/\delta X_1) = 0 \qquad (1)$$

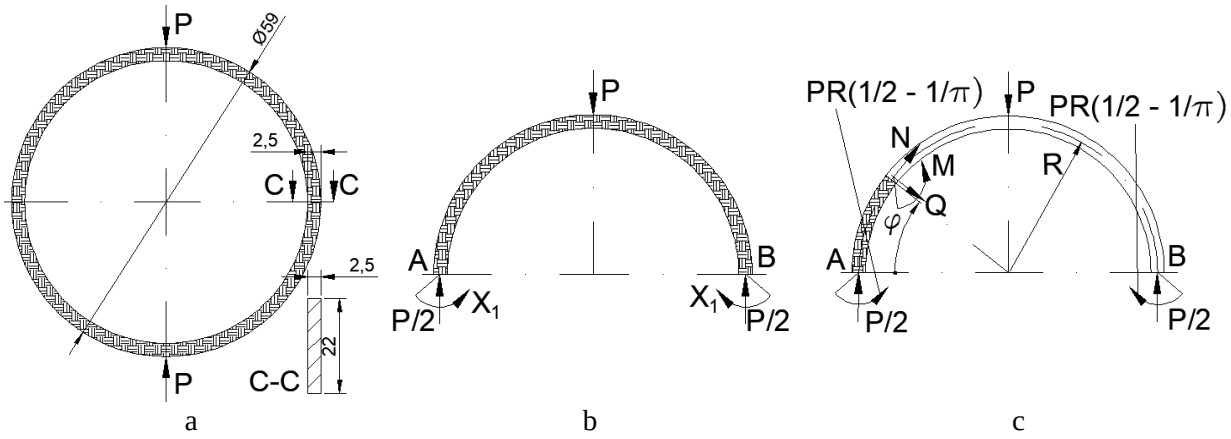

a b c

Figure 4. Thin ring: **a)** Dimensions and load scheme; **b)** Scheme for determining of the staticaly undetermined bending moment X1; **c)** Scheme for determining the internal forces (normal force N, tangential force Q and bending moment M) with respect to the angular coordinate of cross-section φ.

The thin ring (Figure 4-a) is a closed planar contour and is three times statically indetermined [6, page 532] and has two planes of symmetry, both - the horizontal and the vertical (the last is where the two compressive forces P act). If the ring is cut off in the horizontal plane of symmetry and the equilibrium of the upper half (Figure 4-b) is checked, then in the cross-sections (left A and right B) the tangential efforts will be zero because they are antisymmetrical [6, page 524] [5, page 209]. Again, from symmetry with respect to the vertical plane in which the forces P act, it follows that $N_A = N_B = P / 2$ and $M_A = M_B = X_1$. Unknown here will be the moments in cross-sections A and B, denoted by X_1. When considering the equilibrium of the shaded part (Fig. 4-c), the internal forces (normal N, tangential Q and bending moment M) can be expressed in any section as functions of the angular coordinate φ (R is the mean radius of the cross-sections):

$$\Sigma F_{ix} = N + (P/2).\cos\varphi = 0 \quad \therefore\rightarrow \quad N = N(\varphi) = -(P/2).\cos\varphi \qquad (2)$$

$$\Sigma F_{iz} = Q - (P/2).\sin\varphi = 0 \quad \therefore\rightarrow \quad Q = Q(\varphi) = (P/2).\sin\varphi \qquad (3)$$

$$\Sigma M_{iy} = M - (P/2).(R - R.\cos\varphi) + X_1 = 0 \quad \therefore\rightarrow \quad M = M(\varphi) = -X_1 + (PR/2).(1 - \cos\varphi) \qquad (4)$$

The expression of the potential energy of the defformed elastic ring with an unchangeable cross-sections is given by (5) where: F is the cross-sectional area, E - the modulus of elasticity of the ring's material, G - the modulus of the angular deformations of the material, J – the moment of inertia of the cross-section of the ring, k - characteristic constant [6, page 303] of the cross-section which is related to calculating the potential energy of the deformation caused by the tangential internal force Q:

$$U = 4.\{ \int_0^{\pi/2} [N(\varphi)^2/(2.E.F)].R.d\varphi + \int_0^{\pi/2} [k.Q(\varphi)^2/(2.G.F)].R.d\varphi + \int_0^{\pi/2} [M(\varphi)^2/(2.E.J)].R.d\varphi\} \qquad (5)$$

In (5) the integration is performed from 0 to $\pi/2$ radians for one of four similar arcs (all equal to a quarter of a full circle) of the ring and then the result is multiplied by a factor of 4 to obtain the potential energy of the entire ring deformation. For the determination of X_1 he theorem of Menabrea (1) is used, according to which (2), (3), (4) and (5) is obtained (in (6) it should take into account that the partial derivative $\delta M(\varphi)/\delta X_1 = -1 \neq 0$, but $\delta N(\varphi)/\delta X_1 = 0$ and $\delta Q(\varphi)/\delta X_1 = 0$):

$$(\delta U/\delta X_1) = 4. \int_0^{\pi/2} (1/EJ).M(\varphi).(\delta M(\varphi)/\delta X_1) = (4/EJ)\int_0^{\pi/2} (-X_1 + (PR/2).(1 - \cos\varphi))(-1)R.d\varphi = 0 \qquad (6)$$

,where E = const and J = const. From equation (6) for X_1 is obtained:

$$X_1 = (PR).(1/2 - 1/\pi) \qquad (7)$$

Thus the function of the change of the bending moment M from (4) is obtained:

$$M = (PR/2).(2/\pi - \cos\varphi) \qquad (8)$$

Characteristic - deflection of the ring's diameter with respect of the applied load P

After obtaining the expressions of the internal forces N, Q and M as functions of the parameter φ in analytical form, the determination of the diameter deflection's (Δ) dependence to the applied load (P) is performed by applying the Castigliano's second theorem [6, page 488], taking into account that $\delta N/\delta P = -(1/2).\cos\varphi$, $\delta Q/\delta P = (1/2).\sin\varphi$ and $\delta M/\delta P = (R/2).(2/\pi - \cos\varphi)$ in the expressions below:

$$\Delta = \delta U/\delta P$$

$$=4.\{\int_0^{\pi/2}[N(\varphi)/(E.F)].(\delta N/\delta P).R.d\varphi+\int_0^{\pi/2}[k.Q(\varphi)/(G.F)].(\delta Q/\delta P).R.d\varphi+\int_0^{\pi/2}[M(\varphi)/(E.J)].(\delta M/\delta P).R.d\varphi\}$$

$$= 4.\{[(P.R)/(4.E.F)].\int_0^{\pi/2}\cos^2(\varphi).d\varphi + [(P.k.R)/(4.G.F)].\int_0^{\pi/2}\sin^2(\varphi).d\varphi + [(P.R^3)/(4.E.J)].[(4/\pi^2).\int_0^{\pi/2}d\varphi - 2.(2/\pi).\int_0^{\pi/2}(\cos\varphi).d\varphi + \int_0^{\pi/2}(\cos^2\varphi).d\varphi]\} \qquad (9)$$

Or:

$$\Delta = (\pi/4).[R/(E.F)].P + (k.\pi/4).[R/(G.F)].P + (2/\pi + \pi/4 - 4/\pi).[R^3/(E.J)].P \qquad (10)$$

The first two addends in (10) generated from N and Q are negligible with respect to the third addend, which is derived from the contribution of the bending moment M, and therefore we can assume that:

$$\Delta \approx (2/\pi + \pi/4 - 4/\pi).[R^3/(E.J)].P = (0.14877839).[R^3/(E.J)].P \qquad (11)$$

This result gives the relationship between the deflection Δ of the diameter of the ring and the applied force P in analytical form and overlaps with the results in [4, page 24], [6, page 508]. The reciprocal of (11) will be the elastic characteristic "Load P - Diameter Change (Deflection) Δ".

THIN PROVING RING WITH NON-CONSTANT CROSS-SECTION

Internal forces induced by load with diametrical compressive forces

Again under the name thin ring is meant a ring (Figure 3-a) whose dimensions in the radial direction of the cross-section are negligible in relation to its diameter. Here, however, the ring has a non-constant cross-section because, although the width b = 22 mm is constant, the other dimension - the thickness h varies from 1 to 2.5 mm through a 90° angle. In addition, this ring has 4 holes ∅6.1 mm (two vertical and two horizontal) to fastening the force-receiving elements, which also cause a non-constant cross-section. Again, to determine the internal forces and the elastic characteristic "Diameter's Deflection Δ - Applied Force P" at load with two opposite, compressive and equal diametrical forces, the general theorems from Strength of Materials are used - the Castigliano's second theorem and the Menabrea theorem. Here again the expressions for the internal forces (normal N, tangential Q and bending moment M) in the cross-section with the angular coordinate φ (it can be used again Figure 4-c) can be given with the expressions (2), (3) and (4), but the mean cross-sectional radii R = R (φ) and axial moment of inertia of the cross-section J = J (φ) are no longer constants, but they change with respect of φ. This makes it practically impossible to solve analytically way the integrals from (6) for determining the moment X_1 in the cross-sections A and B and the integrals from (9) for determining the deflection Δ of the diameter. For this a numerical integration by means of trapezium rule was applied here using the Microsoft Excel program (Figure 5), with predefined characteristics R = R (φ) and J = J (φ) at a step of an interval of a δφ = 5° angle step.

	A	B	C	D	E	F	G	H	I	J	K	L	M	N	O	P	Q	R	S	T	U	
1											I1		I2		I3					IntM1	IntM2	IntM3
2																						
3	fi [deg]	fi [rad]	Rs [m]	Rb [m]	Rav [m]	h [m]	b [m]	J [m^4]	fi cp[rad]	Jcp [m^4]		Rav/J [cp]		Rav*cosFi/J		COS(fi)	COS^2(fi)	SIN^2(fi)	R^3(fi)/J(fi)			
4	0	0	0.027	0.0295	0.02825	0.0025	0.016	2.08E-11				1.36E+09		1.36E+09		1	1	0	1082172.75			
5	5	0.087266	0.027	0.0295	0.02825	0.0025	0.01859	2.42E-11	0.043633	2.25E-11	110090093	1.17E+09	3.1100E+06	1.16E+09	3.1046E+06	0.996194698	0.992403877	0.007596123	931402.0441	4.55304E-08	4.28579E-07	4.27
6	10	0.174533	0.02715	0.0295	0.028325	0.00235	0.022	2.38E-11	0.1309	2.4E-11	102868255	1.19E+09	2.9099E+06	1.17E+09	2.8821E+06	0.984807753	0.96984631	0.03015369	955134.9436	4.25437E-08	4.0154E-07	3.5
7	15	0.261799	0.027495	0.0295	0.028498	0.002005	0.022	1.48E-11	0.218166	1.93E-11	136149990	1.93E+09	3.8710E+06	1.86E+09	3.7669E+06	0.965925826	0.933012702	0.066987298	1567262.79	5.63082E-08	5.3688E-07	5.0
8	20	0.349066	0.027795	0.0295	0.028647	0.001705	0.022	9.09E-12	0.305433	1.19E-11	221653412	3.15E+09	6.3372E+06	2.96E+09	6.0179E+06	0.939692621	0.883022222	0.116977778	2585165.763	9.16702E-08	8.83824E-07	7.97
9	25	0.436332	0.028045	0.0295	0.028772	0.001455	0.022	5.65E-12	0.392699	7.37E-12	359551135	5.09E+09	1.0328E+07	4.61E+09	9.4917E+06	0.906307787	0.821393805	0.178606195	4213909.181	1.48701E-07	1.44715E-06	1.22
10	30	0.523599	0.028242	0.0295	0.028871	0.001258	0.022	3.65E-12	0.479966	4.65E-12	567093314	7.91E+09	1.6351E+07	6.85E+09	1.4417E+07	0.866025404	0.75	0.25	6590382.08	2.34535E-07	2.29964E-06	1.78
11	35	0.610865	0.028385	0.0295	0.028942	0.001115	0.022	2.54E-12	0.567232	3.1E-12	841301058	1.14E+10	2.4325E+07	9.32E+09	2.0392E+07	0.819152044	0.671010072	0.328989928	9527994.039	3.47941E-07	3.43072E-06	2.47
12	40	0.698132	0.028471	0.0295	0.028985	0.001029	0.022	2E-12	0.654498	2.27E-12	1129297712	1.45E+10	3.2712E+07	1.11E+10	2.5822E+07	0.766044443	0.586824089	0.413175911	12188147.4	4.67049E-07	4.62217E-06	2.88
13	45	0.785398	0.0285	0.0295	0.029	0.001	0.022	1.83E-12	0.741765	1.92E-12	1323185463	1.58E+10	3.8363E+07	1.12E+10	2.8208E+07	0.707106781	0.5	0.5	13303090.91	5.47236E-07	5.42568E-06	2.93
14	50	0.872665	0.028471	0.0295	0.028985	0.001029	0.022	2E-12	0.829031	1.92E-12	1323185463	1.45E+10	3.8363E+07	9.32E+09	2.5947E+07	0.64278761	0.413175911	0.586824089	12188147.4	5.47236E-07	5.42568E-06	2.48
15	55	0.959931	0.028385	0.0295	0.028942	0.001115	0.022	2.54E-12	0.916298	2.27E-12	1129297712	1.14E+10	3.2712E+07	6.52E+09	2.0033E+07	0.573576436	0.328989928	0.671010072	9527994.039	4.67049E-07	4.62217E-06	1.7
16	60	1.047198	0.028242	0.0295	0.028871	0.001258	0.022	3.65E-12	1.003564	3.1E-12	841301058	7.91E+09	2.4325E+07	3.95E+09	1.3219E+07	0.5	0.25	0.75	6590382.08	3.47941E-07	3.43072E-06	1.01
17	65	1.134464	0.028045	0.0295	0.028772	0.001455	0.022	5.65E-12	1.090831	4.65E-12	567093314	5.09E+09	1.6351E+07	2.15E+09	7.6808E+06	0.422618262	0.178606195	0.821393805	4213909.181	2.34535E-07	2.29964E-06	5.10
18	70	1.22173	0.027795	0.0295	0.028647	0.001705	0.022	9.09E-12	1.178097	7.37E-12	359551135	3.15E+09	1.0328E+07	1.08E+09	4.0474E+06	0.342020143	0.116977778	0.883022222	2585165.763	1.48701E-07	1.44715E-06	2.24
19	75	1.308997	0.027495	0.0295	0.028498	0.002005	0.022	1.48E-11	1.265364	1.19E-11	221653412	1.93E+09	6.3372E+06	4.99E+08	1.9678E+06	0.258819045	0.066987298	0.933012702	1567262.79	9.16702E-08	8.83824E-07	8.67
20	80	1.396263	0.02715	0.0295	0.028325	0.00235	0.022	2.38E-11	1.35263	1.93E-11	136149990	1.19E+09	3.8710E+06	2.07E+08	8.7657E+05	0.173648178	0.03015369	0.96984631	955134.9436	5.63082E-08	5.3688E-07	2.84
21	85	1.48353	0.027	0.0295	0.02825	0.0025	0.01859	2.42E-11	1.439897	2.4E-11	102868255	1.17E+09	2.9099E+06	1.02E+08	3.8088E+05	0.087155743	0.007596123	0.992403877	931402.0441	4.25437E-08	4.0154E-07	7.6
22	90	1.570796	0.027	0.0295	0.02825	0.0025	0.016	2.08E-11	1.527163	2.25E-11	110090093	1.36E+09	3.1100E+06	2.19E-06	1.2538E+05	1.61557E-15	2.61007E-30	1	1082172.75	4.55304E-08	4.28579E-07	1.50
23											9582380861		2.7661E+08		1.8838E+08					3.96303E-06	3.89524E-05	1.94
24																						
25	dfi [rad]=	0.087266																		DeltaMcoef =	1.39065E-06	
26	X1 za P=1	0.004604																				

Figure 5. Microsoft Excel program for determining the moment X_1 in the cross-sections A and B and the deflection of the diameter Δ by means of numerical integration.

Because of that the expression (6) is recorded in such way:

$$(\delta U/\delta X_1) = (4/E)\{X_1.\int_0^{\pi/2}[R(\varphi)/J(\varphi)].d\varphi - (P/2).\int_0^{\pi/2}[R^2(\varphi)/J(\varphi)].d\varphi + (P/2).\int_0^{\pi/2}[R^2(\varphi).\cos\varphi/J(\varphi)].d\varphi\} = 0 \quad (12)$$

Integrals from (12):

$$I_1 = \int_0^{\pi/2}[R(\varphi)/J(\varphi)].d\varphi \quad (13)$$

$$I_2 = \int_0^{\pi/2}[R^2(\varphi)/J(\varphi)].d\varphi \quad (14)$$

$$I_3 = \int_0^{\pi/2}[R^2(\varphi).\cos\varphi/J(\varphi)].d\varphi \quad (15)$$

are solved numerically by means of the trapezium rule and then is found X_1.

$$X_1 = [(I_2 - I_3)/I_1].(P/2) \quad (16)$$

About function of the change of the bending moment with respect of φ from (4) and (16) it is obtained:

$$M = (P/2).[(I_2 - I_3)/I_1 - R(\varphi) + R(\varphi).\cos\varphi)] \quad (17)$$

Characteristic - deflection of the ring's diameter with respect of the applied load P

Again, the determination of the dependence of the deflection of the diameter □ - the applied load P is performed by applying the Castigliano's second theorem [6, page 488], and again it should take into account that $\delta N/\delta P = -(1/2).\cos\varphi$, $\delta Q/\delta P = (1/2).\sin\varphi$, but here from (17) follows:

$$\delta M/\delta P = (1/2).[(I_2 - I_3)/I_1 - R(\varphi) + R(\varphi).\cos\varphi)] \quad (17)$$

That way the expression for determination of Δ is obtained as:

$$\Delta = \delta U/\delta P = 4.(P/4).\{(1/E).\int_0^{\pi/2}[R(\varphi)/F(\varphi)].\cos^2(\varphi).d\varphi + (k/G).\int_0^{\pi/2}.[R(\varphi)/F(\varphi)].\sin^2(\varphi).d\varphi + (1/E).[((I_2 - I_3)/I_1)^2.\int_0^{\pi/2}[R(\varphi)/J(\varphi)].d\varphi + \int_0^{\pi/2}[R^3(\varphi)/J(\varphi)].d\varphi + \int_0^{\pi/2}[R^3(\varphi).\cos^2(\varphi)/J(\varphi)].d\varphi + 2.[((I_2-I_3)/I_1).\int_0^{\pi/2}[R^2(\varphi).\cos(\varphi)/J(\varphi)].d\varphi]-((I_2-I_3)/I_1).\int_0^{\pi/2}[R^2(\varphi)/J(\varphi)].d\varphi-\int_0^{\pi/2}[R^3(\varphi).\cos(\varphi)/J(\varphi)].d\varphi]\}$$

In the above expression, the integrals are solved by numerical integration by means of trapezium rule. If we neglect the part of Δ, which arises from the internal forces N and Q (and the numerical results have shown that their share is one hundred times smaller than the one generated by the bending moment M), then for deflection Δ it could enroll:

$$\Delta = (P/E).[((I_2 - I_3)/I_1)^2.\int_0^{\pi/2}[R(\varphi)/J(\varphi)].d\varphi + \int_0^{\pi/2}[R^3(\varphi)/J(\varphi)].d\varphi + \int_0^{\pi/2}[R^3(\varphi).\cos^2(\varphi)/J(\varphi)].d\varphi + 2.[((I_2-I_3)/I_1).\int_0^{\pi/2}[R^2(\varphi).\cos(\varphi)/J(\varphi)].d\varphi]-((I_2-I_3)/I_1).\int_0^{\pi/2}[R^2(\varphi)/J(\varphi)].d\varphi-\int_0^{\pi/2}[R^3(\varphi).\cos(\varphi)/J(\varphi)].d\varphi]\}$$

In the case of a selected material 40X for the ring according to the Russian standard (the American analogue is AISI 1045 Steel with $E = 2.05.10^{11}$Pa and $G = 8.10^{10}$Pa) after numerical integration from the above expression, the relationship between Δ in m and P in N is obtained as:

$$\Delta = 1.39065.10^{-6}.P, \text{ m} \quad (18)$$

3-D MODELLING OF THE PROVING RING BY MEANS OF CAD

To verify and to compare the results of the above dependence (18), a 3-D model (Figure 6-a) of the dynamometer proving ring it have been constructed by means of the CAD software product SolidWorks 2013 according to the geometric dimensions of Figure 3. Then, using the embedded package Simulation which uses the finite element method, the deflections (Figure 6-c) of the vertical diameter under load according to Figure 4-a, as well as the Von Mises equivalent stresses, were examined. The results are summarized in Table 1 and in graphical way (Figure 8).

EXPERIMENTAL EXAMINATION

The proving ring (Figure 3-b) is made from steel 40X (Russian standard)) and has been loaded by means of a special spring testing machine (Figure 7-a). Reading of load is done by the indicator of the testing machine, and the ring diameter deflections was measured by means of dial indicator for linear measuring mounted in the ring. The results are summarized in Table 1 and graphical way (Figure 8).

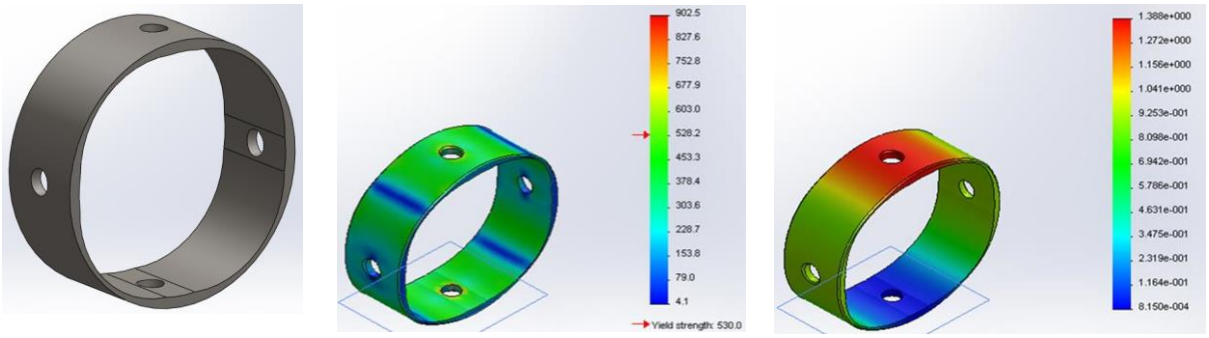

a b c

Figure 6. a) 3-D model, **b)** Von Mises equivalent stresses at P=1000 N, **c)** deflections at P=1000 N.

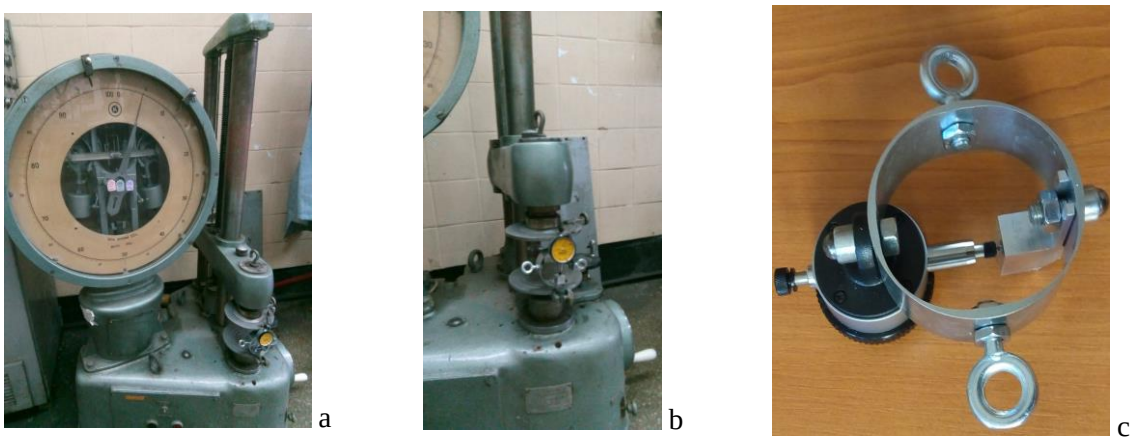

a b c

Figure 7. Experimental tests - a) spring testing machine, b) ring attachment, c) attaching the dial indicator for linear measuring to the ring.

RESULTS AND DISCUSSION

Table 1 summarizes the results obtained: by means of the theoretical investigation, by means of the simulation of loading of the 3-D model in the SolidWorks 2013 in CAD environment and by means of the experimental tests.

Table 1. Results - theoretical, from 3-D model and experimental

Non Experimental	3-D model	After Castigliano	Experimental	
Load P, N	Deformation Δ, mm		Load P, N	Deformation Δ, mm
0	0	0	0	0
100	0.1388	0.139065084	98.0665	0.15
200	0.2775	0.278130169	196.133	0.29
300	0.4163	0.417195253	294.1995	0.45
400	0.555	0.556260338	392.266	0.6
500	0.6938	0.695325422	490.3325	0.79
600	0.8325	0.834390506	588.399	0.95
700	0.9713	0.973455591	686.4655	1.13
800	1.11	1.112520675	784.532	1.3
900	1.249	1.25158576	882.5985	1.48
1000	1.388	1.390650844	961.0517	1.64

These results are illustrated in Figure 8. It is seen that theoretical rasults and results derived by means of 3-D modeling practically coincide. The experimental results are close to the theoretical and the ones obtained by means of modeling, but the steepness of the experimental "deformation - load" dependence is greater and that steepness of this dependence increases when the loading increases. The

reasons for this deviation should be sought in the imperfection of the experimental system: the way of loading application, the way of load reading, the way the ring is attached, etc. Other possible sources are the deviations of the actual dimensions of the ring and of the deviation of the elasticity parameters of the material (E and G) from those of the theoretical or model ones, the deviation of the actual axis of measurement from theoretical axis, influence of the attachment of the dial indicator for linear measuring on the characteristics of the ring itself, etc.

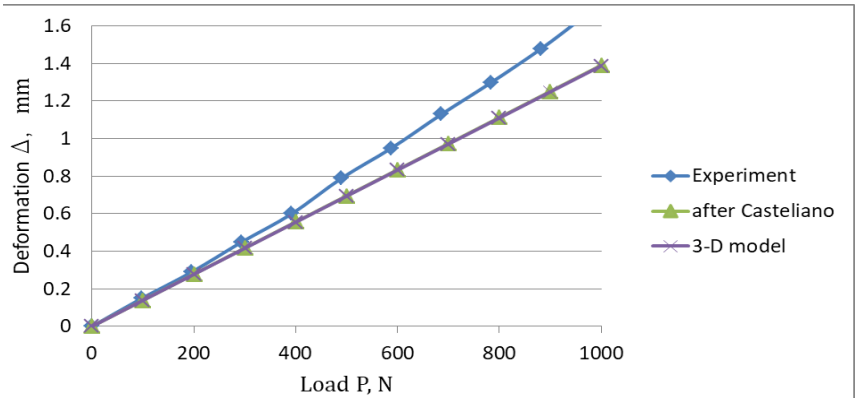

Figure 8. Graphs of the dependences "deflection Δ - loading P".

CONCLUSION

The proving rings with variable cross-sectional geometry are more difficult for theoretically deriving of the "diametrical deformation - diametrical load" dependence. This can be done by applying the general theorems from Strength of Materials, and by means of using numerical integration of expressions derived from these theorems because of the variable geometry of the cross section of these rings. The other easier approach is the use of modern methods of 3-D modeling and load simulation software. Here it is shown that this is achievable on one and the other approach, and the results are comparable. The experimental results concerning the dependence "Diametrical Deflection - Diametrical Load" are relatively close to theoretical and these from modeling, the difference being explained by the deviations of the parameters of the dynamometric ring as geometry and material from those of the theoretical and modeling studies as well as the imperfections of the experimental research.

REFERENCES

[1] Josué Njock Libii, Design, analysis and testing of a force sensor for use in teaching and research World Transactions on Engineering and Technology Education UICEE Vol.5, No.1, pp.175 – 178, 2006.
[2] https://www.nist.gov/pml/quantum-measurement-division/mass-and-force/proving-ring-design
[3] Bill Schweber, The Proving Ring: How Innovation Led to a Simple Tool to Verify Weight, 19 May 2015, https://insights.globalspec.com/article/987/the-proving-ring-how-innovation-led-to-a-simple-tool-to-verify-weight.
[4] Hvorslev Mikael J., Notes on proving rings and frames for soil testing equipment, Army Engineer Waterways Experiment Station Vicksburg, Mississippi, March 1972
[5] Феодосиев В.И., Сопротивление материалов, Наука, Главная редакция физико-математической литературы, Москва 1979 г.
[6] Кисьов Иван Д., Съпротивление на материалите, Държавно издателство „Техника“, V-то издание, София, 1978 г.
[7] Орлов П.И., Основы конструирования, Книга I, Москва, Машиностроение, 1988 г.
[8] Rahman M. Ashiqur, Rahman Sharifur, Design parameters of a circular proving ring of uniform strength,Proceedings of the International Conference on Mechanical Engineering 2005 (ICME2005) 28-30 December 2005, ICME05-AM-15, Dhaka, Bangladesh.